Available online at www.sciencedirect.com
ScienceDirect
Coordination Chemistry Reviews 251 (2007) 2592–2605
COORDINATION CHEMISTRY REVIEWS
www.elsevier.com/locate/ccr

Review

Direct observation of crystalline-state guest exchange in coordination networks

Masaki Kawano *, Makoto Fujita *

Department of Applied Chemistry, School of Engineering, The University of Tokyo, and CREST, Japan Science and Technology Agency (JST), 7-3-1 Hongo, Bunkyo-ku, Tokyo 113-8656, Japan

Received 29 December 2006; accepted 27 July 2007
Available online 6 August 2007

Contents

Abstract

This review describes the recent investigations, within the last several years, of single-crystal-to-single-crystal transformations of coordination networks on guest-removal/inclusion processes. Single-crystal diffraction analyses reveal intriguing features of coordination networks such as robustness, dynamic framework transformations, biporous formation and specific molecular recognitions, gas absorption, induction of intermolecular interactions between host and guest and so on. The atomic level information provides a deeper insight into the correlation of unique physicochemical properties with crystal structures.
© 2007 Elsevier B.V. All rights reserved.

Keywords: Coordination networks; Single-crystal-to-single-crystal reaction; Guest exchange; In situ observation; Host–guest

1. Introduction

Porous coordination networks prepared via self-assembly of a metal (a connector) and a ligand (a link) have attracted considerable attention because of their ease of systematic modification and tunability and unique physicochemical properties such as separation, catalytic reaction, magnetism, gas uptake, and so on. Another salient feature is that, unlike zeolites, many coordination networks often form single crystals suitable for single-crystal diffraction analysis, allowing correlation of physical properties with atomic level structure. Therefore, syntheses, structural characterization, and physicochemical properties of networks have been extensively investigated in the past decade [1]. The breakout of organic–inorganic hybrid coordination network compounds is partially derived from the

* Corresponding authors. Tel.: +81 3 5841 7204; fax: +81 3 5841 7257.
E-mail addresses: mkawano@appchem.t.u-tokyo.ac.jp (M. Kawano), mfujita@appchem.t.u-tokyo.ac.jp (M. Fujita).

0010-8545/$ – see front matter © 2007 Elsevier B.V. All rights reserved.
doi:10.1016/j.ccr.2007.07.022

expectation for porous post-zeolite materials since the early 1990s [2]. Advance in detector technology brought about commercially available charge-coupled detector or an imaging plate capable of fast data collection and prompt detectability of diffraction change owing to crystal decay or phase transition. One can now collect highly redundant data quickly, which produces higher and sharper electron density peaks resulting in good data. That means that disordered guest molecules can be more clearly observed. Thanks to such advantages of high performance area detectors, one can perform in situ experiments more readily. In situ crystallography is extremely powerful to characterize guest exchange reactions in a coordination network in solid–liquid or solid–gas phases. It is indispensable for developing tailor-made functional materials to obtain a deeper understanding of unique guest-triggered phenomena. Several excellent comprehensive reviews on coordination networks have been published [1], so in this review we focus on single-crystal-to-single-crystal reactions in coordination networks reported in the past several years from a crystallographic point of view.

2. In situ crystallography

In situ crystallography has been utilized for the characterization of crystalline-state photoreactions for more than 30 years [3]. The advantage of the method is that under the same conditions one can directly observe the trace of molecular motions induced by reactions in a crystal and often reveal the reaction mechanism on a basis of structural information. In the case of a coordination network, there are several difficulties in obtaining useful results: guest molecules are sometime statistically or dynamically disordered because of a large and fluid cavity; guest exchange suffers from crystal decay or generation of multi-crystals, and so on [4]. Therefore, an important starting point for in situ crystallography is as accurate preliminary knowledge of chemical formula of a crystal as possible. The use of chemical constraints to model severely disordered guest molecules is useful but special care is necessary when applying constraints to thermal temperature factors. The proper temperature factors should be used to model molecules missing expected electron density peaks. If the model is not correct, the thermal temperature factor will diverge and the refinement will not stably converge. However, one should carefully follow crystallographic basic steps for successful modeling. In situ crystallographic analysis is a common technique, but the model determined by in situ crystallographic analysis should always be confirmed by other spectroscopic methods, i.e. IR spectroscopy.

3. Features of coordination networks

A coordination network consists of a metal (a connector) and a ligand (a link) where coordination bonds play a crucial role in the self-assembly and flexibility of the framework. Because the coordination bond can be labile in solution, metals and ligands can readily reorganize in solution, leading to thermodynamically or kinetically stable conformers. An organic–inorganic hybrid porous network is not as tough as zeolite, but it has the fascinating characteristics of a flexible framework. Dynamics induced by the flexibility should correlate with the physical properties and functions. In general, dynamic behavior in porous materials has been investigated by spectroscopic rather than crystallographic methods, but recently many intriguing phenomena in a crystal have been reported. In the next section the recent work of single-crystal-to-single-crystal reactions in a coordination network are discussed.

4. Single-crystal-to-single-crystal transformations

4.1. Robust networks—single-crystal-to-single-crystal guest removal

The robustness of a porous coordination network is an important factor for the industrial use in separations and catalysis. In general, the coordination network is not as robust as zeolite, however, in the early, several very robust networks were reported.

In 1999, Kepert and Rossensinsky first elucidated the rigid coordination network, $[Ni_2(4,4'\text{-bipy})_3](NO_3)_4\cdot 6EtOH$ (**1**), by single-crystal X-ray diffraction [5]. The interlocked bilayer framework has 6 Å × 3 Å channels parallel to the *a*-axis which can reversibly take up H_2O at room temperature with other guests such as EtOH, MeOH, and *i*-PrOH. The crystal structures of **1** before and after desolvation were determined (Fig. 1). Surprisingly, the desolvation process at 375 K causes just a 2.4% decrease in cell volume and the mosaicity of the crystal retains intact. The average shift of atomic position in the framework is 0.06 Å. These facts illustrate the robustness of the framework in **1**.

At the same time, Williams et al. also reported a robust coordination network, $[Cu_3(\text{benzene-1,3,5-tricarboxylate})_2]\cdot 3H_2O$ (**2**) with 9 Å × 9 Å square-shaped pores (Fig. 2) [6]. The material **2** is thermally stable to 513 K, but no desolvated crystal structure of **2** was reported. The salient feature of **2** is its chemical functionalizability. The axial aqua ligands can be exchanged for other ligands, i.e. pyridine, and the metal is also replaceable, i.e. by Os. The ability to readily modify the metals and ligands of coordination networks is in sharp contrast to zeolites.

In 1999 Yaghi and co-workers also reported an exceptionally stable and highly porous metal–organic framework, $[Zn_4O(BDC)_3]\cdot(DMF)_8(C_6H_5Cl)$ (**3**; DBC = 1,4-benzenedicarboxylate; DMF = *N*,*N*′-dimethylformamide) [7]. The framework is so robust that a fully dehydrated structure can be characterized by single-crystal X-ray analysis as well. The salient feature of the network is its gas-uptake capability, which is described in detail in Section 4.8.

In 2000 we reported an open 20 Å × 20 Å square-grid coordination network, $[Ni(4,4'\text{-bis(4-pyridyl)biphenyl})_2](NO_3)_2\cdot(o\text{-xylene})$ (**4**) [8]. The 2D layer of **4** was prepared via self-assembly of a rod-like ligand, 4,4′-bis(4-pyridyl)biphenyl, with $Ni(NO_3)_2$ in *o*-xylene. The framework has amazing thermal stability and maintains its integrity up to 573 K. We succeeded in determining the crystal structure of the desolvated **4** as well. The dynamic

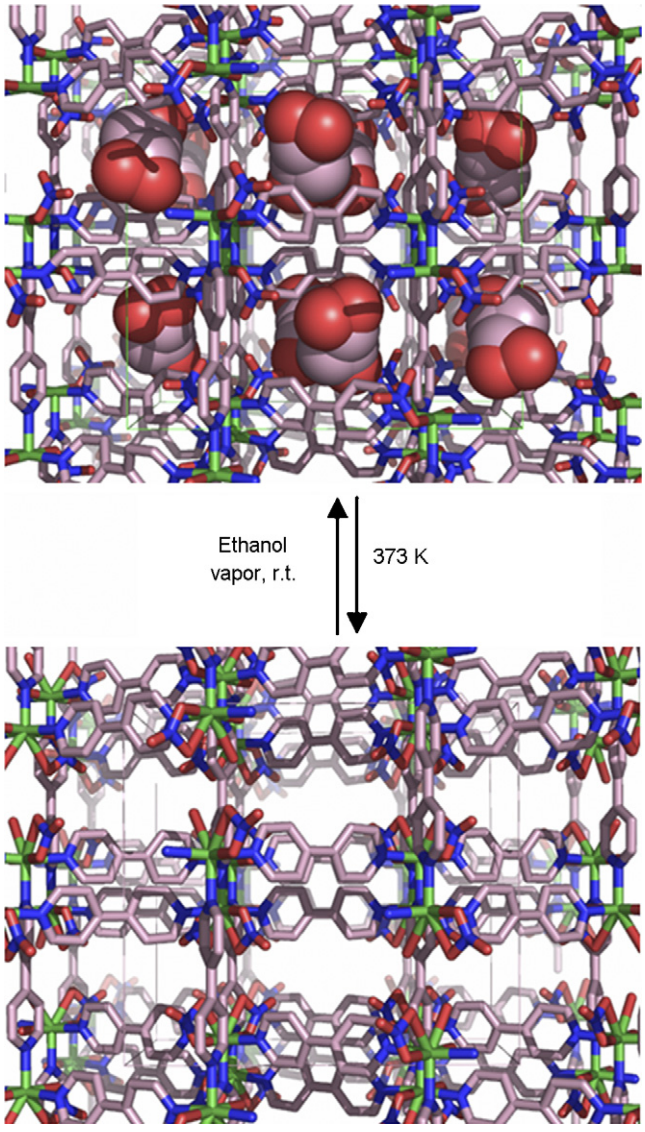

Fig. 1. Guest inclusion/removal in **1** viewed down the *a*-axis: Ni, green; O, red; N, blue; C, pink. Ethanol molecules (space-filling model) are disordered.

motion of the framework on guest exchange is described in Section 4.2.

In 2005 Hosseini and co-workers prepared a crystal of a robust zinc-porphyrin-based coordination network which shows reversible single-crystal-to-single-crystal transformation upon guest removal and/or exchange (Fig. 3a and b) [9]. The ligand design concept is based on the directionality of a porphyrin ring and metal coordination sites. Crystals of the 3D hexagonal network, **5**-Zn·X (**5** = 5,15-di(4-pyridyl)-10,20-diphenylporphyrin; X = MeOH or EtOH; Fig. 3c) were prepared from slow diffusion of a $CHCl_3$ solution of **5** into a MeOH or EtOH solution of $Zn(OAc)_2{\cdot}2H_2O$. The framework is composed of interconnected porphyrin rings containing hexagonal channels filled with disordered MeOH or EtOH molecules.

The robustness of the **5**-Zn framework facilitated the determination of the empty framework structure (Fig. 3d) as well as a structure where the guest solvent molecules were exchanged.

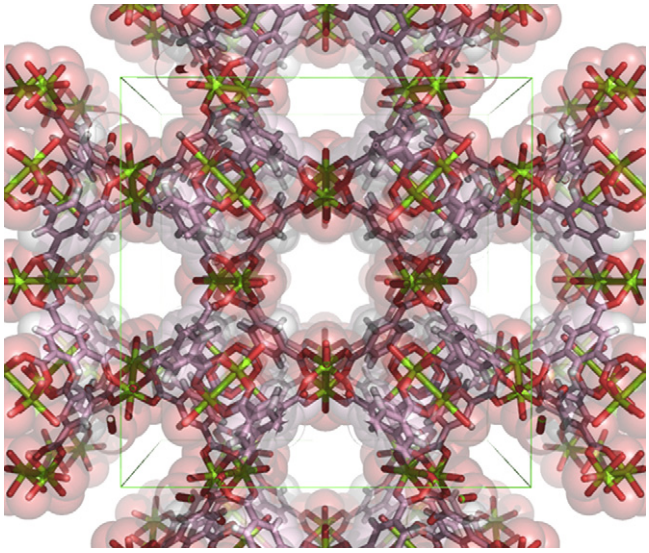

Fig. 2. Crystal structure of **2** viewed down the *a*-axis: Cu, green; O, red; C, pink. For clarity solvent is omitted.

4.2. *Flexible networks—single-crystal-to-single-crystal guest removal/exchange*

In contrast to robust systems, two groups reported in 2002 the first single-crystal-to-single-crystal guest exchange reactions, highlighting the highly flexible nature of network compounds. Suh et al. reported the synthesis of a porous bilayer-open-framework, $[Ni_2(C_{26}H_{52}N_{10})]_3[BTC]_4{\cdot}6C_5H_5N{\cdot}36H_2O$ (**6**), which was prepared from the reaction of dinickel(II) bismacrocyclic complex $[Ni_2(C_{26}H_{52}N_{10})](Cl)_4{\cdot}H_2O$ (Fig. 4) and sodium 1,3,5-benzenetricarboxylate (Na_3BTC) in water in the presence of DMSO and pyridine. The network **6** retains its framework and the single crystallinity upon removal and uptake of guest molecules [10]. Their synthetic strategy is based on the construction of 3D channels in a bilayer framework consisting of robust 2D nickel(II) layers and flexible pillars as shown in Fig. 5. The crystal shows sponge-like dynamic motion, reducing the interlayer spacing dramatically in response to guest removal involving rotation, swing, and bending motions to produce $[Ni_2(C_{26}H_{52}N_{10})]_3[BTC]_4{\cdot}4H_2O$ (**6′**). During the transformation of **6** into **6′**, no practical change was observed in the 2D layers (the cavities of size 22.2 Å × 14.4 Å), but the thickness of the bilayer was greatly reduced from 11.91(1) Å to 6.82(2) Å, due to significant tilting of the pillars. The void volume of 61% in **6** significantly decreased to 27% in **6′**.

When the single crystal **6′** was exposed to water–pyridine vapor for 12 h or immersed in water–pyridine mixture for 5 min, it returned to **6** as demonstrated by powder X-ray diffraction patterns. In 2006 a modified compound, $[Ni(cyclam)]_2[BPTC]{\cdot}2H_2O$ (cyclam = 1,4,8,11-tetraazacyclotetradecane; BPTC = 1,1′-biphenyl-2,2′,6,6′-tetracarboxylic anion), was also reported. The diffusion of water molecules into the dehydrated nonporous structure is very slow (ca. 5 days), probably because of the drastic conformational change of the framework [11].

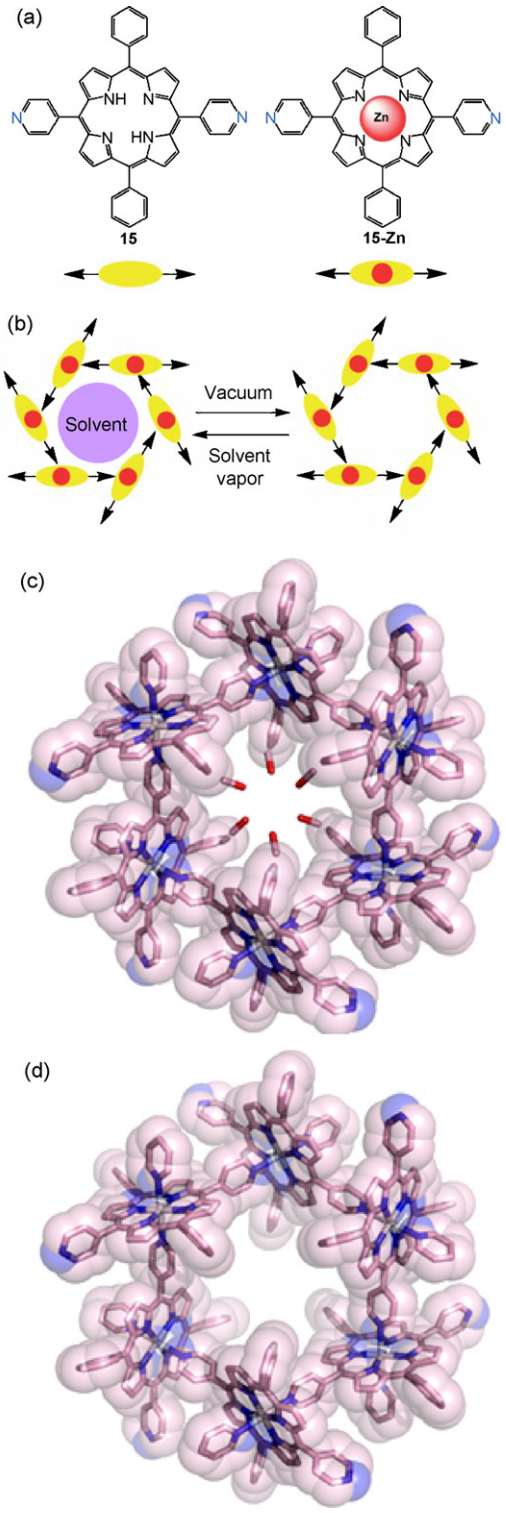

Fig. 3. Zinc-porphyrin-based porous network: (a) self-assembled units, (b) schematic representation of the guest exchange, (c) the crystal structure of 3D hexagonal network, **5**-Zn·MeOH, and (d) that of the empty cage after vacuum.

Our group reported a 3D network structure, $[(ZnI_2)_3(TPT)_2]\cdot 6C_6H_5NO_2$ (**7**), assembling from ZnI_2 and TPT (2,4,6-tris(4-pyridyl)triazine) in nitrobenzene (or cyanobenzene) and methanol [12,13]. The doubly interpenetrated 3D network of **7** shrinks on guest removal and swells on guest encapsulation without loss of crystallinity (Fig. 6). In network **7**, the 3D framework (green in Fig. 7) and the inversion-center-related one (tint in Fig. 7) interpenetrate, and generate a robust framework flexible enough to accommodate guest exchange in a single-crystal-to-single-crystal fashion. For example, crystals of **7** show a remarkable ability to exchange nitrobenzene for various organic molecules such as benzene, mesitylene, *cis*-stilbene, and $CHCl_3$ without deterioration of crystallinity. Fig. 8 shows a packing of encapsulated benzene in the channel of **7** instead of nitrobenzene which reflects on the large size of channel. Interestingly, the crystal data became better on guest exchange of nitrobenzene for benzene because of better packing of benzene within the channels of **7** ($R_1 = 5.5\%$ versus 7.9%).

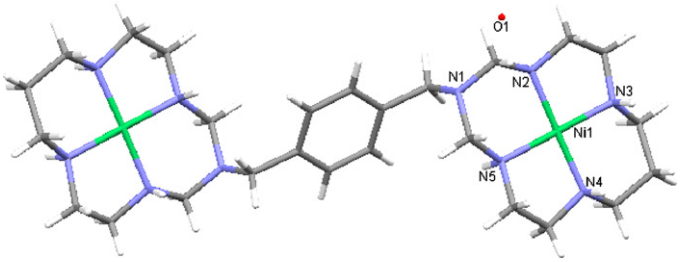

Fig. 4. Molecular structure of a dinickel(II) bismacrocyclic complex in $[Ni_2(C_{26}H_{52}N_{10})](PF_6)_4\cdot H_2O$.

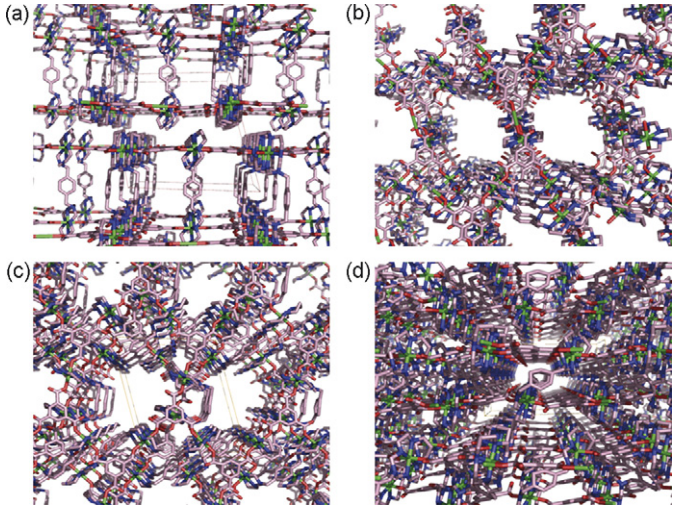

Fig. 5. Crystal structures of **6** and **6′**. (a) **6** viewed down in the (1 0 0) direction, (b) **6** viewed down in the (1 0 1) direction, (c) **6′** viewed down in the (1 0 0) direction, and (d) **6′** viewed down in the (0 1 0) direction.

Desolvated crystals (**7′**), were prepared by leaving crystals of **7** at room temperature to equilibrate with atmosphere for a day. Crystallographic analysis of **7′** revealed that the monoclinic

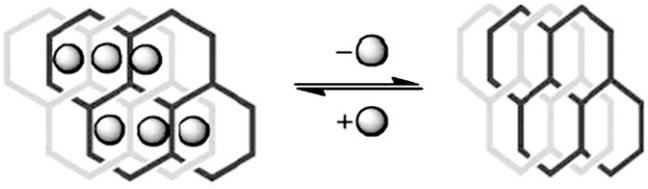

Fig. 6. Schematic representation of the contraction/expansion of an interpenetrated network on guest removal/inclusion.

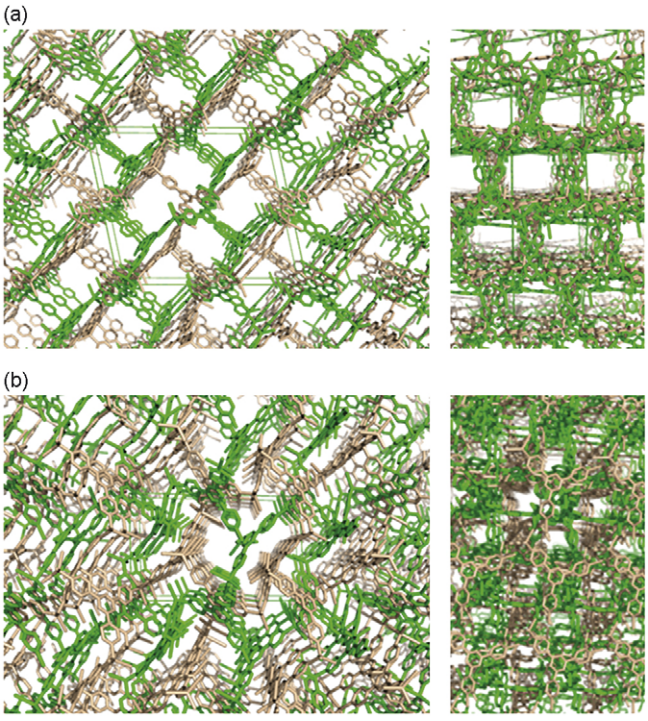

Fig. 7. Crystal structures of **7** and **7′**. (a) View of **7**: left, in the (0 1 0) direction; right, in the (1 0 1) direction; a nitrobenzene inclusion framework. (b) View of the desolvated framework **7′**: left, in the (0 1 0) direction; right, in the (1 0 1) direction.

crystal system of **7** changes into triclinic in **7′** and the framework considerably compresses (Fig. 7b) [14]. The void volume of 61% in **7** decreases to 23% in **7′**. When crystals of **7′** were placed in nitrobenzene for a day, the network re-expands to **7** while retaining crystallinity. These results demonstrate the robustness and flexibility of the interpenetrated framework of **7**.

Our group also reported single-crystal-to-single-crystal sliding of 2D coordination layers of **4** having 20 Å × 20 Å square grids [15] triggered by guest exchange (Fig. 9) [16]. The crystals of **4** showed guest specificity and exchanges of *o*-xylene for mesitylene but not for *m*-xylene, or 1,3- or 1,2-dimethoxybenzene. The crystals of a mesitylene-inclusion network, $[Ni(4,4'\text{-bis(4-pyridyl)biphenyl})_2](NO_3)_2\cdot 1.7(\text{mesitylene})$ (**4a**), were prepared by immersion of **4** in mesitylene for 6 h. The single-crystal analysis of **4a** revealed considerable sliding of the layers relative to the 2D framework of **4** (Fig. 10). Edge-to-face aromatic interactions exist at the corner of the channels in both **4** and **4a** but not along the walls. The dimensions of the channels in **4a** are much bigger than that of **4**. The sliding motion of the 2D layers could be monitored by X-ray powder and single-crystal diffraction. The crystallographic results and

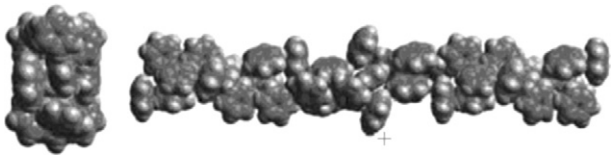

Fig. 8. Space-filling representation of benzene molecules aligned in the channel after guest exchange in **7** (top and side views).

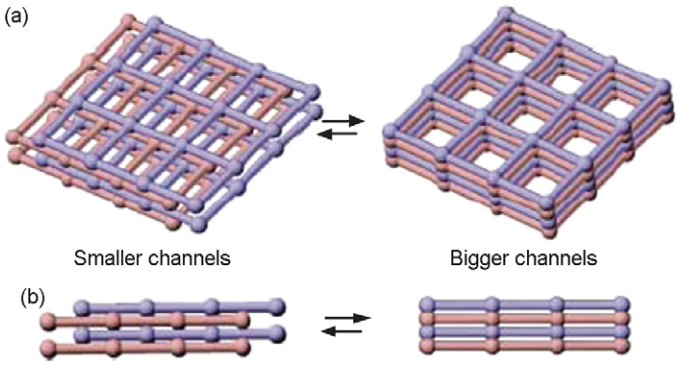

Fig. 9. Sliding motion of 2D layers: (a) top and (b) side views.

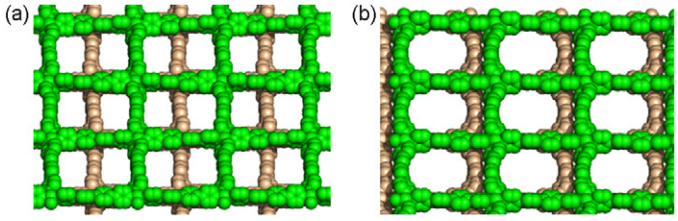

Fig. 10. Packing of 2D layers in (a) **4** and (b) **4a** viewed down the *c*-axis. Solvent molecules are omitted for clarity.

GC analysis clearly indicate that the framework transformation proceeds in a crystal-to-crystal fashion. The first step is guest exchange and the second step is the sliding of the layers.

In 2004 Kitagawa and co-workers found the unexpected expanding of porous networks, $[Cd(pzdc)(azpy)(NO_3)_2\cdot 2H_2O]$ (**8**) (pzdc = pyrazine-2,3-dicarboxylate) and $[Cd(pzdc)(bpee)(ClO_4)_2\cdot 1.5H_2O]$ (**9**) on guest removal [17]. The isostructural networks, **8** and **9**, were formed according to the scheme in Fig. 11. The key contributions to the unique transformation are electronic repulsive forces and attractive hydrogen bonding interactions. When the water molecules in **8** were completely removed at 403 K (Fig. 12b), the cell volume increases significantly. In contrast to **8**, the interlayer distance in **9** decreases on the basis of PXRD. The expansion in **8** is attributed to

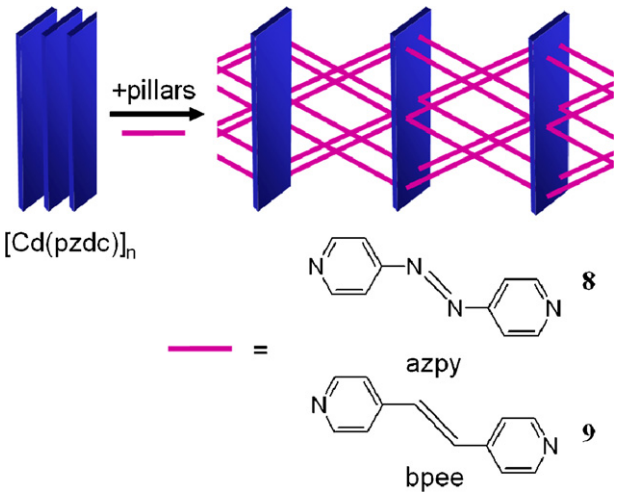

Fig. 11. Schematic representation of the network formation of **8** and **9**.

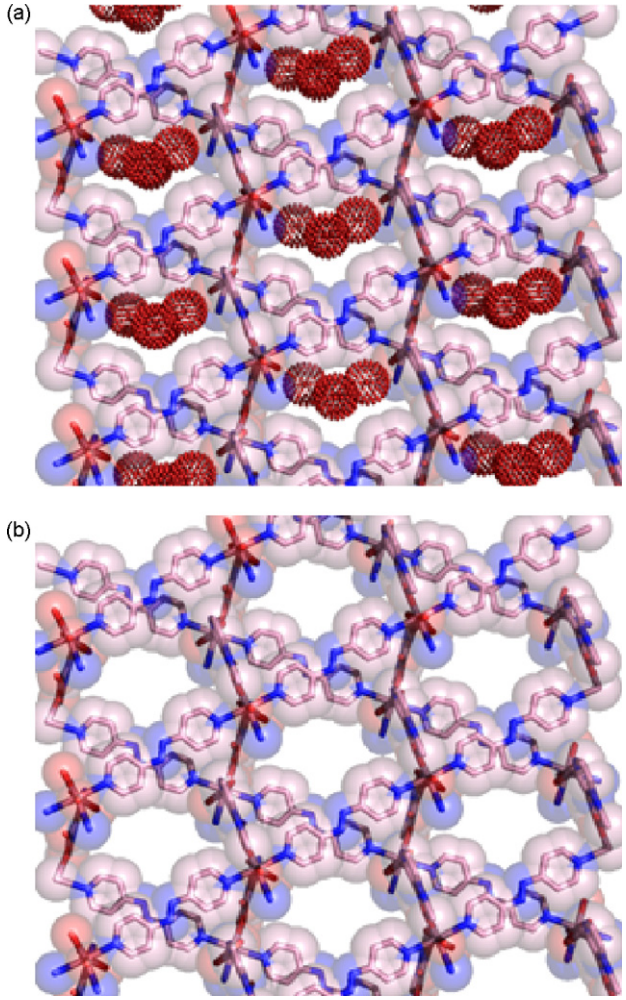

Fig. 12. Crystal structures of the two-layer stack of **8** viewed down the *c*-axis: (a) before and (b) after the complete dehydration (**8′**). Dot spheres in (a) indicate water oxygen atoms.

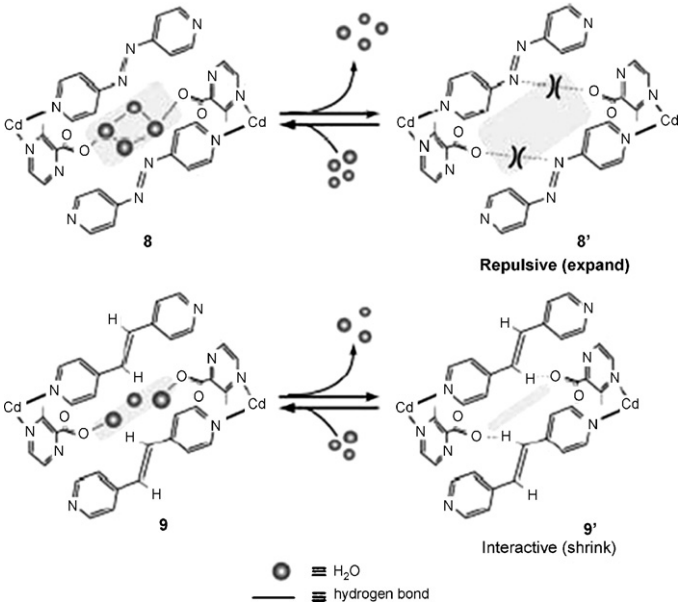

Fig. 13. Mechanism for expansion and shrinking of **8** and **9** on water removal.

lone pair–lone pair electronic repulsion between pendant oxygen atoms of the carboxylate and the nitrogen atoms of the azo group. The compression of **9** is induced by hydrogen bonding interactions between pendant oxygen atoms and ethylene hydrogen atoms (Fig. 13). The dehydrated **9** selectively adsorbs H_2O, MeOH, THF, and Me_2CO at 298 K but not N_2 even at 77 K, irrespective of whether or not guests are similar in size.

In 2005, Halder and Kepert reported an in situ crystallographic study of desorption and sorption of solvent in flexible porous coordination networks, $[Co_2(4,4'\text{-bipy})_3(NO_3)_4\cdot(\text{guest})]$ (guest: EtOH, MeOH, $Me_2C{=}O$, MeCN, THF, CH_2Cl_2), in the cobalt analogue of **1** [18]. Their studies indicate what the origin of flexibility of the coordination network is. Diffraction studies revealed intra- and inter-bilayer flexible motions in the framework and the presence of hydrogen bonding networks between the host and guest molecules. Electron density maps were used to give a more informative image of the disordered guest molecules within the host channels.

In 2005 Suh reported a robust, flexible porous coordination network, $[Zn_4O(NTB)_2]\cdot 3DEF\cdot EtOH$ (**10**), which was prepared by the solvothermal reaction of $Zn(NO_3)_2\cdot 6H_2O$ and 4,4′,4″-nitrilotrisbenzoic acid (H_3NTB) in DEF/EtOH/H_2O [19]. The framework possesses remarkable thermal stability (up to 703 K) with retaining porosity. The framework sustains single crystallinity even at 673 K under vacuum. The network shows a reversible rotation on guest removal and rebinding (Fig. 14). Additionally, the framework possesses multifunctionality, i.e. selective organic guest binding and guest-dependent blue luminescence. Compound **10** shows high hydrogen gas storage capability.

4.3. Coordination-mode change in frameworks—single-crystal-to-single-crystal guest removal/exchange

In the course of study of 2D-layered network systems having square grids, we designed a linear bidentate pyridyl ligand having ethylene glycol side chains to generate a robust, flexible coordination network [20]. Slow complexation of $Co(NO_3)_2\cdot 6H_2O$ in MeOH with the rod-like ligand L in toluene produced orange-yellow single crystals of $[Co(L)_2(H_2O)_2](NO_3)_2\cdot 1.5H_2O$ (**11**) in 76% yield (Eq. (1)). X-ray analysis revealed that the 2D-layered network contained square-grid sheets with an infinite 1D hydrogen bonding network through the channels of the layers (Fig. 15). In sharp contrast to the framework with no ethylene glycol chains, the framework in **11** is significantly stabilized against thermal destruction by the hydrogen bonding networks. Thanks to the thermal stability, we could perform in situ crystallographic study on desorption and sorption processes of water guest molecules in **11**. We could directly observe a reversible apical-ligand-exchange reaction at the hinge metals (Fig. 16). Upon heating at 423 K the yellow crystal of **11** turned red with no loss of crystallinity. X-ray analysis revealed that the apical water molecules were substituted by two nitrate ions and extruded from the crystal to produce empty channels. Upon exposure of the dehydrated

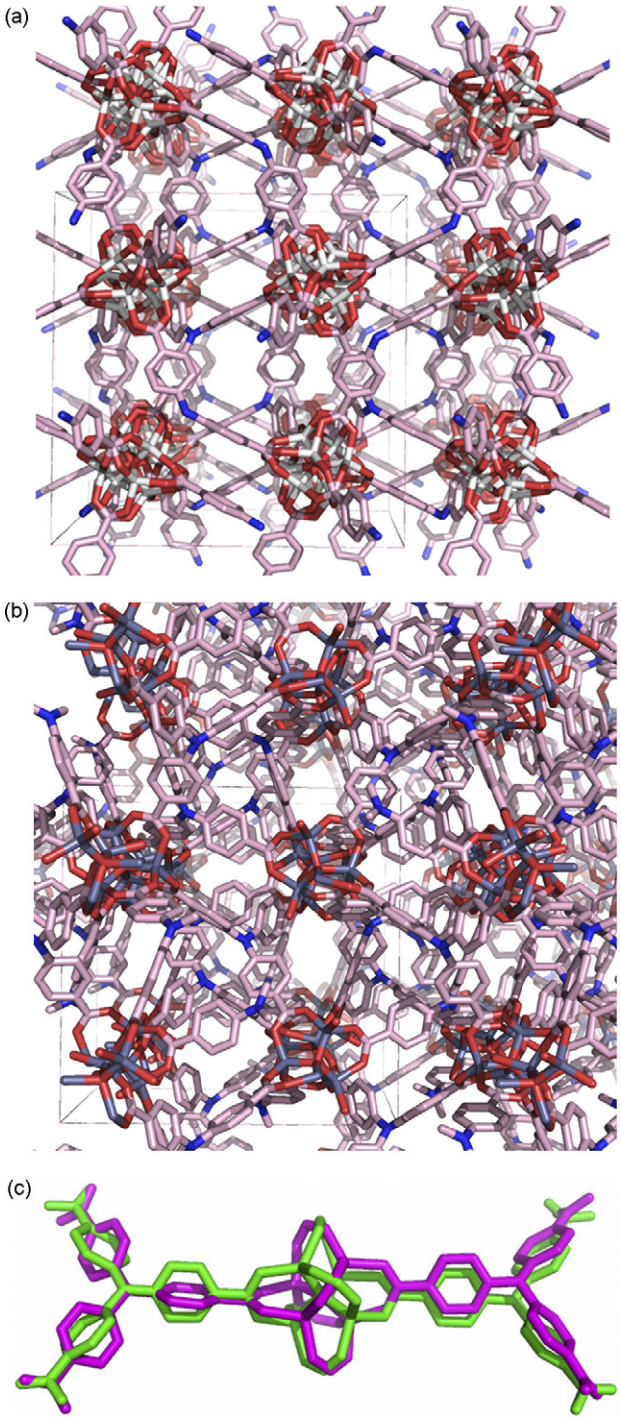

Fig. 14. Crystal structures of the robust as well as flexible porous coordination network of **10**: (a) before desolvation and (b) after desolvation. Color code in (a) and (b): Zn, grey; O, red; N, blue; C, pink. (c) Rearrangements of the framework components: before desolvation, green; after desolvation, pink. Removal of the guest molecules resulted in a significant amount of rotation occurring in the remaining framework structure.

network (**11′**) to air at room temperature, the color of the crystal returned to yellow within a few minutes without any deterioration of crystallinity. We performed spectroscopic and magnetic studies and elucidated that the chromism accompanied with guest sorption and desorption can be ascribed to a change in the

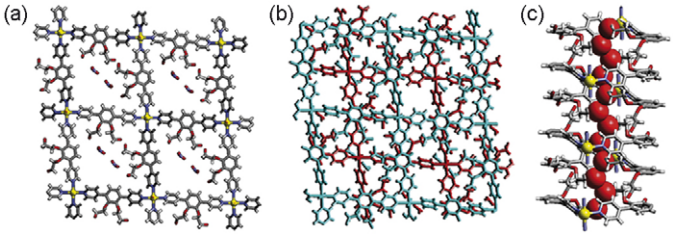

Fig. 15. Crystal structures of 2D-layered network **11** viewed down the *c*-axis. Water molecules are omitted for clarity. (a) The square-grid framework, (b) the two-layer stack, and (c) the infinite 1D hydrogen bond (O–H···O) array in **11**.

energy levels of the d-orbitals of cobalt, induced by apical-ligand exchange:

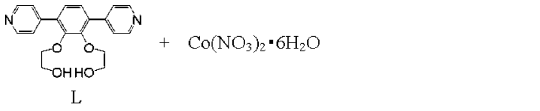

(1)

In 2004 Sevov and co-workers reported a dynamic reversible transformation of a zinc polycarboxylate network in crystalline state driven by production of low coordination mode of Zn by dehydration [21]. Although this review is not intended to cover inorganic networks, their single-crystal-to-single-crystal work deserves a brief mention. Porous networks of $[Co_2L(H_2O)_2]\cdot 2.33H_2O$ (**12**) and $[Zn_3L(OH)_2(H_2O)_{1.33}]\cdot 3H_2O$ (**13**) (L = tetrahydrofuran-2,3,4,5-tetracarboxylic acid, referred to as THFTCA or H_4L) were prepared by the reaction of THFTCA and $CoCl_2$ or $ZnCl_2$, respectively. The major difference is that in addition to the two different metal positions in **12**, compound **13** has an additional third zinc position [22]. The networks have similar rings and narrow channels but additional ZnO_6 octahedra block the channels

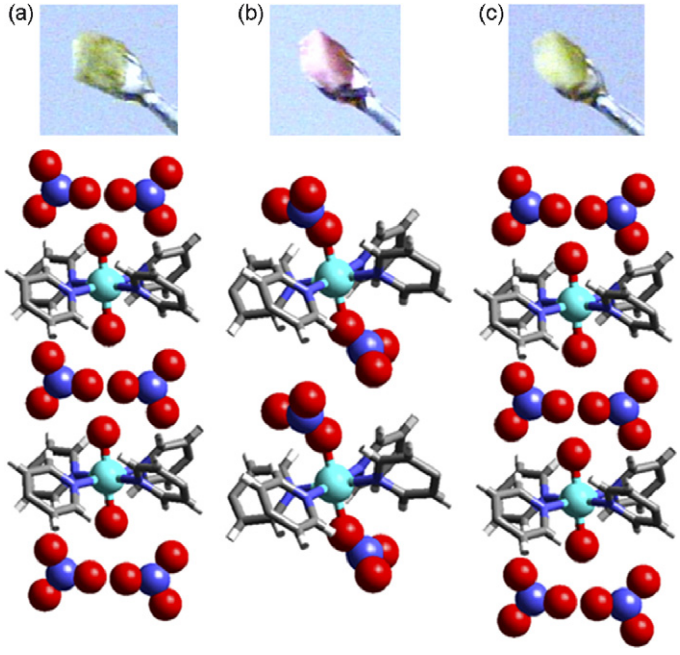

Fig. 16. Structural transformation of **11** depending on temperature: (a) original crystal, (b) after heating at 423 K for 24 h, and (c) after exposure of **11′** to air.

in **13**. Single crystals of **12** can be dehydrated by heating under vacuum. The compound **12** loses all non-coordinated and single-bonded water above 443 K to produce blue-purple $Co_2L(H_2O)$ (**12′**) and reversibly rehydrates on exposure to air for a few days. Surprisingly, when heated above 443 K under vacuum, **13** not only loses water, but the extra zinc atoms lose all water and OH ligands and move to a new position 3 Å away. The driving force of the structural transformation may be the stabilization of very low coordinated Zn^{2+} ions generated by ligand loss. Moreover the dehydrated **13** can be partly (68%) converted to the initial structure **13′** again on exposure to air at room temperature after 2 days. Such metal hopping motions are rare in porous coordination network systems.

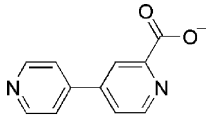

ppca

In 2005 zur Loye and co-workers reported stepwise reversible single-crystal-to-single-crystal transformations of a mixed-metal 3D porous coordination polymer, $[Co_2(ppca)_2(H_2O)(V_4O_{12})_{0.5}]\cdot 3.62H_2O$ (**14**) (ppca = 4-(pyridin-4-yl)pyridine-2-carboxylic acid) on removal of the guest water molecules [23].

Their interesting observation based on high-quality X-ray diffraction data is a conformational change about the cobalt center with a concomitant color change. Small, red, block-shaped crystals of **14** were obtained by hydrothermal reactions of Hppca, $Co(NO_3)_2\cdot 6H_2O$, and NH_4VO_3 in a 1:1:1 ratio at 433 K for 48 h. The network **14** shows a temperature-dependent two-step dehydration (Fig. 17). The first dehydration of **14** at 423 K causes a decrease in volume (from 15% to 12% of the total crystal volume) producing $[Co_2(ppca)_2(H_2O)(V_4O_{12})_{0.5}]\cdot 0.55H_2O$

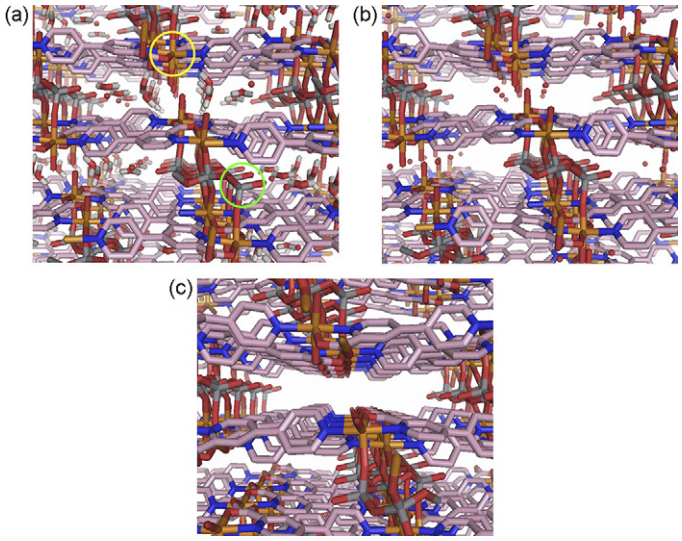

Fig. 17. Crystal structural changes of **14** upon guest removal viewed down the *a*-axis: (a) **14** (before dehydration), yellow circle, a Co unit; green circle, a VO_4 unit, (b) **14′** (after partial dehydration at 423 K), and (c) **14″** (after complete dehydration at 573 K). The dehydration and rehydration processes among **14**, **14′**, and **14″** are reversible. (For interpretation of the references to color in this figure legend, the reader is referred to the web version of the article.)

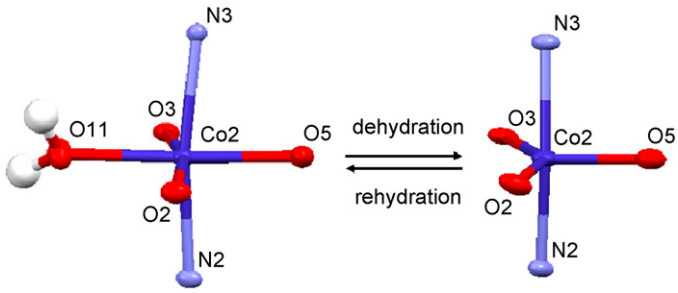

Fig. 18. Conformational change about the cobalt atom from octahedral (in **14** and **14′**) to trigonal bipyramidal (**14″**) on dehydration and rehydration processes.

(**14′**). The second dehydration removes all non-coordinated and coordinated water molecules in **14′** at 573 K to produce $[Co_2(ppca)_2(V_4O_{12})_{0.5}]$ (**14″**). The cobalt ions change from an octahedral to a trigonal bipyramidal coordination (Fig. 18), and the crystal turns from red to brown. Whereas **14″** remains almost isostructural with **14** and **14′**, the unit-cell volume is further decreased and the channels reduce to one-third of their original volume. Immersion of crystals of both **14′** and **14″** in water results in complete rehydration and re-formation of the original structure.

The geometrical transformation of metal centers and coordinatively unsaturated metal formation can be applied to supplement another function to porous materials.

4.4. Single-crystal-to-single-crystal exchange of large guests

In 2004 we reported the single-crystal-to-single-crystal guest exchange of large organic molecules within the porous 3D coordination network, $[(ZnI_2)_3(TPT)_2]$ (**7**), resulting in induction of charge-transfer (CT) interaction between host and guest [24]. Previously, guests, in general, investigated for single-crystal-to-single-crystal guest exchange have been limited to only small molecules, such as solvent, mostly because of small channel sizes. However, the effective inclusion of large molecules as well as the crystallographic observation of the inclusion process is essential to the design of sophisticated functional materials.

The large pores of **5** are filled by nitrobenzene columns (Fig. 19a). When single crystals of **5** are immersed in a saturated cyclohexane solution of triphenylene at room temperature for 24 h, the crystal color of **5** turns pale yellow. The crystals show no change in size and morphology and, after isolation, diffract well for single-crystal X-ray study. The crystallographic analysis revealed the structure of the inclusion complex $[(ZnI_2)_3(TPT)_2]\cdot 1.5(\text{triphenylene})\cdot 2.5(\text{cyclohexane})$ (Fig. 19b). Despite the inclusion of the large guest, the 3D network remains unchanged, and the cell parameters are almost the same as those of **5**. The guest molecule of triphenylene is found in three independent positions A, B, and C as shown in Fig. 19b. In positions B and C, the distance between triphenylene and TPT is ca. 3.4 Å slightly shorter than the sum of van der Waals radii (3.5 Å). Likewise, anthracene and perylene also replace nitrobenzene in **5** to give the inclusion com-

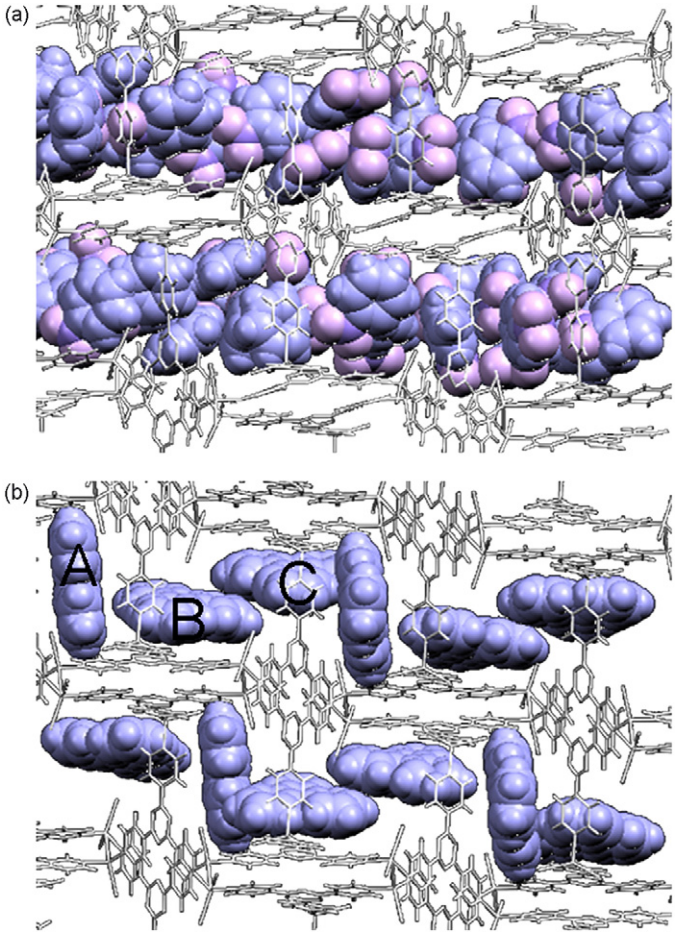

Fig. 19. Crystal structures of **5** viewed down the *b*-axis: (a) before guest exchange (nitrobenzene are encapsulated in the channels) and (b) after guest exchange for triphenylene. Cyclohexanes are omitted for clarity.

plexes $[(ZnI_2)_3(TPT)_2]\cdot 1.4(\text{anthracene})\cdot 2.2(\text{cyclohexane})$ and $[(ZnI_2)_3(TPT)_2]\cdot(\text{perylene})\cdot(\text{cyclohexane})\cdot 1.5(\text{nitrobenzene})$, respectively, without loss of crystallinity. Crystallographic analysis showed efficient π-stacking of the guest and ligand. Close ligand–guest contact suggests donor–acceptor interaction between electron-rich guests and the electron-deficient TPT ligands and was supported by UV–vis studies. DFT calculations also show that the symmetry of the guest HOMOs effectively match the LUMO of the simplified model framework of **5** (Fig. 20). The inclusion complexes of planar aromatic guest with CT interactions are distinctly

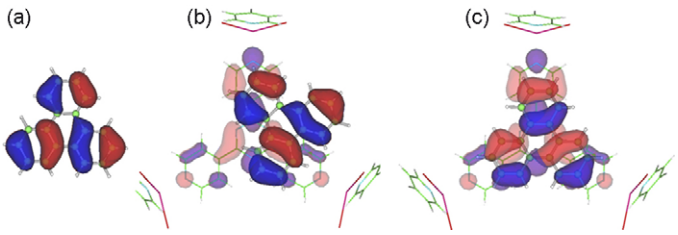

Fig. 20. (a) The HOMO of triphenylene. (b) Superposition of the HOMO of triphenylene and the LUMO of the simplified model framework of **5** in the position B. (c) Superposition of the HOMO and the LUMO in the position **C**.

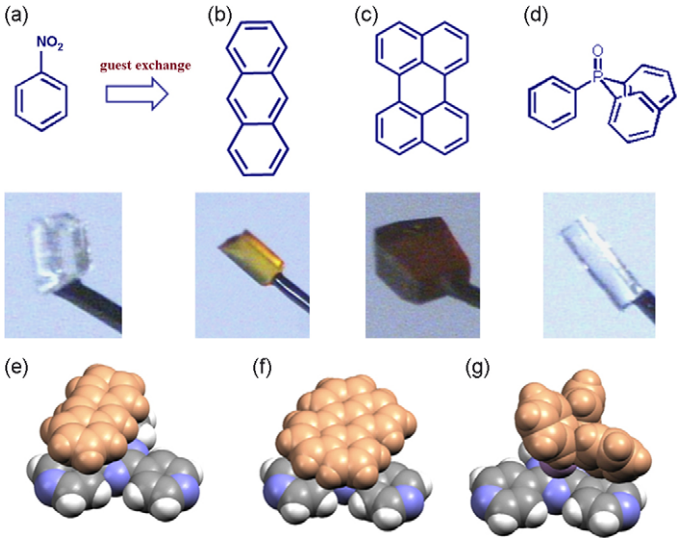

Fig. 21. Crystal color changes of **5** on guest exchange: (a) nitrobenzene, (b) anthracene, (c) perylene, and (d) triphenylphosphine oxide. The partial structures of the inclusion compounds: (e) anthracene, (f) perylene, and (g) triphenylphosphine oxide.

colored whereas the inclusion complex of triphenylphosphine oxide is colorless due to the absence of CT interaction (Fig. 21).

The X-ray characterization of intermolecular interactions will aid the design of not only new inclusion complexes but also incorporation of new physical properties and chemical reactions within the coordination network.

4.5. Specific guest exchange by a biporous network

In 2004 we reported preparation of a biporous coordination network and selective encapsulation of guest into two distinct channels [25]. Prior to this study, most porous coordination networks had uniform channels. If two (or more) distinct channels exist in a crystal, they may take up two (or more) guests independently. Such biporous materials make, for example, the simultaneous isolation or transportation of two different guests possible.

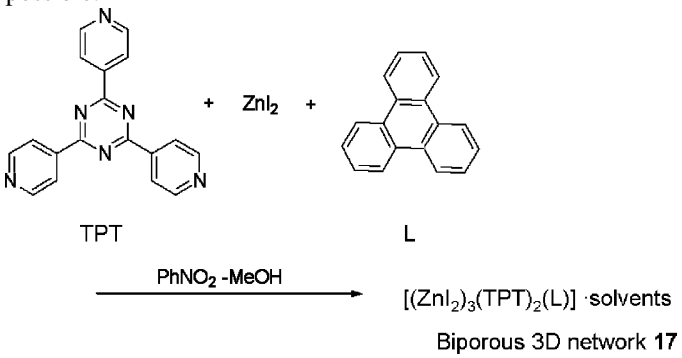

Single crystals of $[(ZnI_2)_3(TPT)_2(L)]\cdot x(\text{nitrobenzene})\cdot y(\text{methanol})$ (**15**; L = triphenylene, $x \approx 4$, $y \approx 2$) were grown from a triple-layered solution with a methanol solution (0.5 mL) of ZnI_2 (0.03 mmol) as the top layer, methanol (0.5 mL) as the middle layer, and a nitrobenzene/methanol solution (4:1,

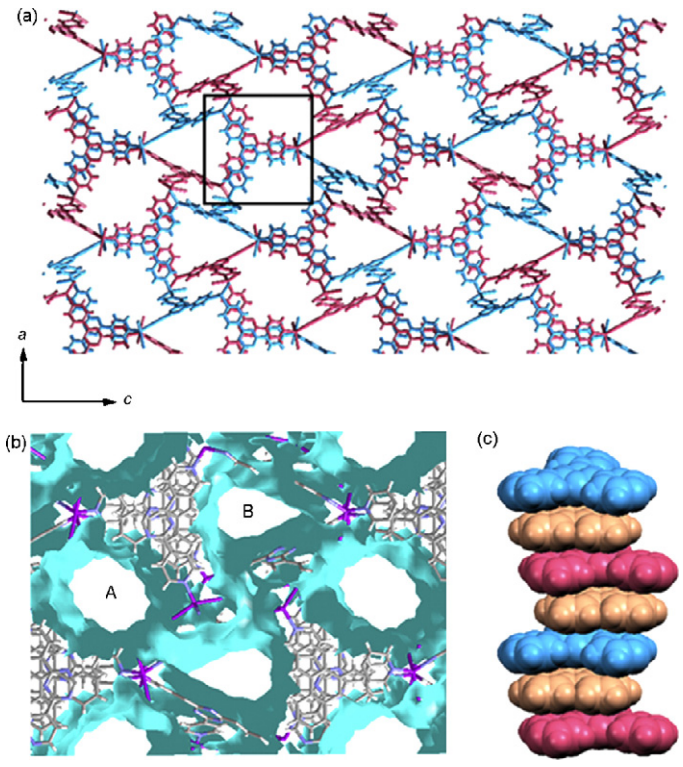

Fig. 22. Crystal structure of **15**: (a) view of the interpenetrated networks along the *b*-axis, (b) two distinct channels A and B, (c) the infinite aromatic stacking between TPT (blue and pink) and triphenylene (orange) at the inserted square in (a). (For interpretation of the references to color in this figure legend, the reader is referred to the web version of the article.)

5 mL) of TPT (0.02 mmol) and triphenylene (L, 0.1 mmol) as the bottom layer. Noteworthy is that triphenylene is best regarded as forming part of the host framework rather than being a guest. The intercalated triphenylene is not replaced by common aromatic compounds under guest exchange conditions because of the strong π–π stacking. The structure of complex **15** contains two distinct channels (A and B) within the framework. Channel A is roughly cylindrical and is lined with the hydrogen atoms of infinitely stacked TPT and L. Channel B, however, is roughly trigonal prismatic, where two of the three walls are the π faces of TPT and the third is the edges of TPT and L (Fig. 22a–c). The approximate dimensions of the channels are 7.4 Å × 5.5 Å (channel A) and 7.3 Å × 5.5 Å (channel B). Surprisingly, the two channels take up their own preferred guests from a mixture: channel A of as-synthesized **15** is filled with nitrobenzene and methanol, which are considerably disordered and could not be fully located by crystallographic analysis, whereas channel B is filled with nitrobenzene (Fig. 23). Dipping crystals of **15** into a saturated cyclohexane solution of naphthalene at room temperature for 2 days caused channels A and B to be selectively filled with naphthalene and cyclohexane, respectively, to give guest exchanged crystals of $[(ZnI_2)_3(TPT)_2(L)]\cdot x(\text{cyclohexane})\cdot y(\text{naphthalene})$ ($x \approx 1.3$ and $y \approx 2.3$). Even after guest exchange, high-quality diffraction data could be collected, and the structure converged to a final R_1 value of 0.052. The crystallographic

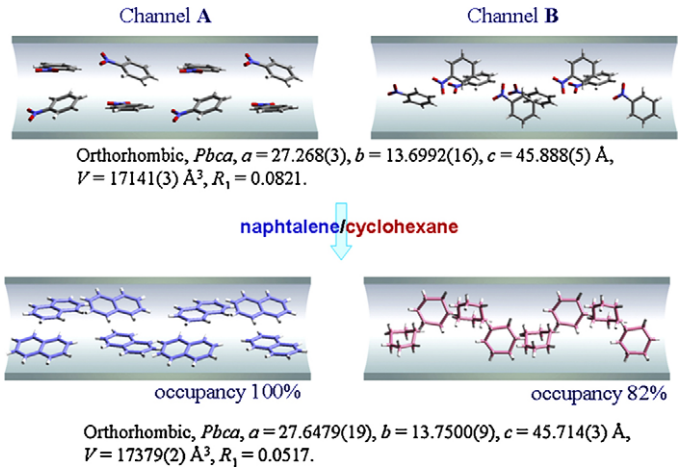

Fig. 23. Selective guest exchange of nitrobenzene for naphthalene and cyclohexane in **15**. Partially disordered molecules are omitted for clarity.

analysis revealed the formation of columnar arrays of naphthalene (100% occupancy) and cyclohexane (82% occupancy) in channels A and B, respectively (Fig. 23). The uptake of two different guests by the two channels was also observed for an azulene/cyclohexane mixture: channels A and B selectively adsorbed azulene (100% occupancy) and cyclohexane (100% occupancy), respectively. A variety of scientific and technological applications are likely to be possible for such a "two-in-one" crystal.

4.6. Control of physical properties via guest exchange

One of the important issues in the field of coordination networks is how to incorporate and control physical properties. The first successful study on magnetic control was reported by Kepert and co-workers in 2002 [26]. A nanoporous coordination network $[Fe_2(azpy)_4(NCS)_4]\cdot(\text{guest})$ (**16**) (azpy = *trans*-4,4′-azopyridine) containing spin-crossover sites was prepared by the slow diffusion of stoichiometric amounts of $Fe^{II}(NCS)_2$ and azpy in ethanol (Fig. 24). Spin-crossover behavior was successfully controlled by both guest removal and sorption. In the presence of guest molecules, 50% of the high-spin Fe atoms became low-spin below 50 K. However, in the absence of guest, no spin-crossover occurred. Moreover, the most notable magnetic behavior is observed by sorption of other solvate molecules

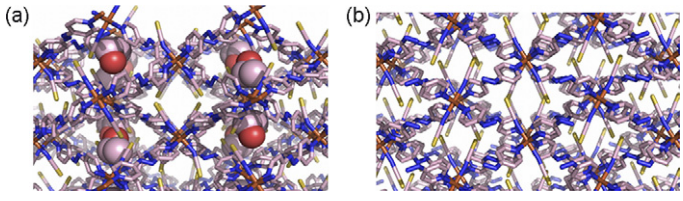

Fig. 24. Crystal structures of **16** viewed along the *c*-axis: (a) the ethanol-inclusion network at 150 K, (b) the desolvated network at 375 K. Framework atoms are represented as sticks and atoms of the ethanol guests as spheres: Fe, orange; S, yellow; O, red; N, blue; C, pink. (For interpretation of the references to color in this figure legend, the reader is referred to the web version of the article.)

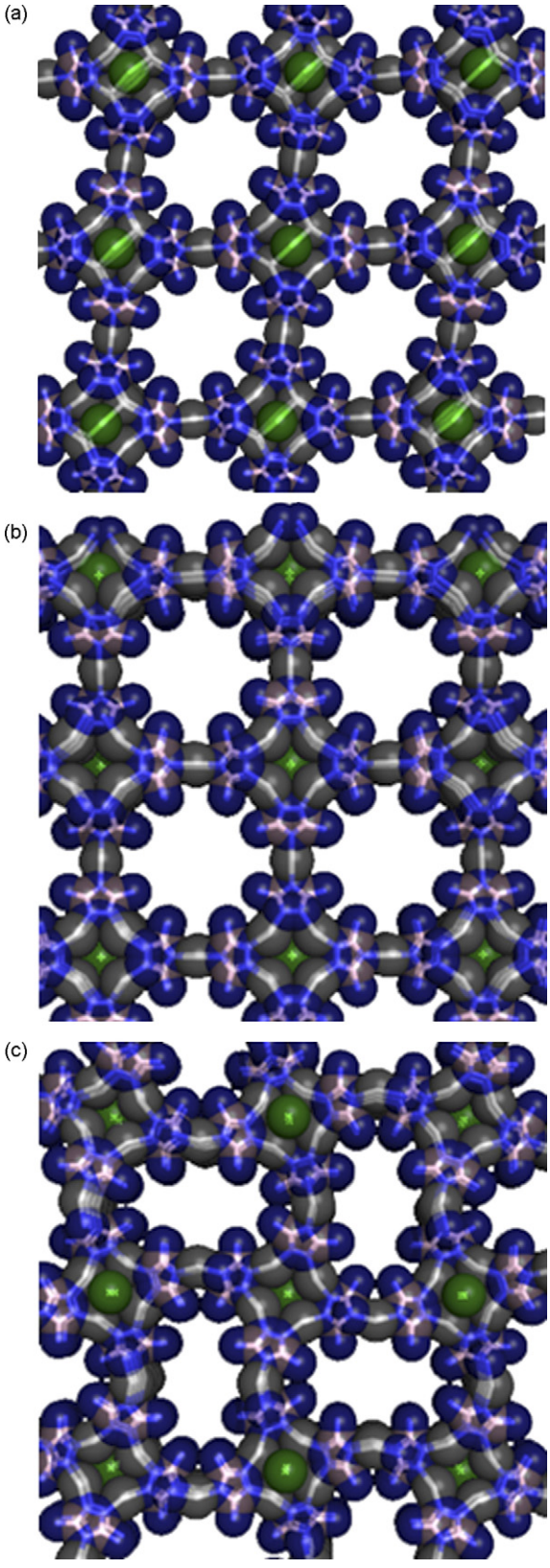

Fig. 25. Framework transformation of **17**: (a) at 103 K (viewed down the *a*-axis), (b) at 293 K (viewed down the *c*-axis), and (c) after dehydration (**17′**) (viewed down the *c*-axis). Solvate molecules are omitted for clarity. Color code: Ag, grey; Cl, green; N, blue; C, pink. (For interpretation of the references to color in this figure legend, the reader is referred to the web version of the article.)

into the empty channels. When the guest is 1-propanol, a clear two-step crossover is observed. The spin dynamics is derived from electronic influence on Fe(II) sites via hydrogen bonding of solvate molecules. The spin-crossover change affects the channel size by decrease/increase of Fe–N bond distances.

4.7. Guest- or temperature-induced framework transformations

In 2005 Chen reported drastic temperature- or guest-induced single-crystal-to-single-crystal transformations of porous coordination network, $[Ag_6Cl(atz)_4]OH{\cdot}6H_2O$ (**17**), prepared by the slow evaporation of an ammonia solution of Hatz (3-amino-1,2,4-triazole) and AgCl [27]. The channels (8.5 Å × 8.5 Å) of the network **17** shows slight elliptical deformation (7.8 Å × 9.2 Å) by changing the temperature from 293 K to 103 K (Fig. 25a and b). Unfortunately, no cell parameters could be determined between 240 K and 120 K. Placing **17** in a very slow stream of dry air or heating at 375 K for 3 h gave the partially desolvated structure **17′**. The channels (4.3 Å × 10.4 Å) of the framework **17′** were dramatically distorted from that of **17** (Fig. 25c). More interestingly, crystallographic analysis provided the evidence for the structural rearrangement of Ag^I–ligand bond cleavages and formations. The dehydration and rehydration process is reversible. Rehydration process is slow, probably because of the structural rearrangement of Ag–ligand.

Wu and Lin reported a porous homochiral coordination network based on 1D polymeric chains and solvent-exchange-induced single-crystal-to-single-crystal transformations [28]. Colorless hexagonal crystals of $[CdL_2(ClO_4)_2]{\cdot}11EtOH{\cdot}6H_2O$ (**18**) (L = (*S*)-2,2′-diethoxy-1,1′-binaphthyl-6,6′-bis(4-vinylpyridine)) were prepared by heating a DMF/*o*-$C_6H_4Cl_2$/EtOH solution of $Cd(ClO_4)_2{\cdot}6H_2O$ with a chiral ligand L at 443 K for 2 days. The 1D chain has a rhombic macrocycle of 19 Å × 19 Å openings, all of which lie parallel to each other in the *ab* plane due to interdigitation (Fig. 26). These layer structures are stabilized by π–π stacking interactions. Treatment with benzene and ethanol vapor resulted in guest exchange. The crystal structures of two phases were determined from the initial structure (space group: $P6_222$). In the first phase ($P6_122$) the network contains the mixture of benzene, ethanol, and water. In the second phase ($P6_222$ again) the network contains benzene and water. The in situ crystallographic analysis clarified that the first intermediate phase is a complicated structure of 1D polymeric chains stacking in an ···ABCDEFABCDEF··· pattern rather than the ···ABCABC··· pattern in **18**. This study is the first example of a chiral coordination network showing a single-crystal-to-single-crystal structural transformation induced by solvent exchange.

4.8. Gas uptake

One of the fascinating properties of coordination networks is gas-sorption ability [6,7,29]. Recent crystallographic studies of gas uptake are briefly summarized in this section.

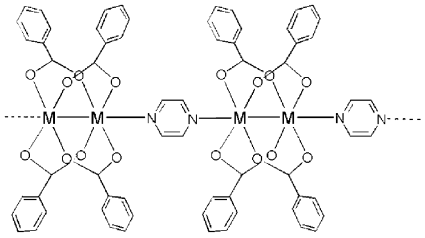

$[Rh^{II}_2(O_2CPh)_4(pyz)]$ (**19**)

The first in situ gas-sorption crystallographic work was reported by Takamizawa et al. using $[Rh^{II}_2(O_2CPh)_4(pyz)]$ (**19**) (pyz = benzoate pyrazine) (Fig. 27a) [30,31]. Several gas-adsorbed crystal structures such as CO_2 and O_2 were determined using the 1D network, **19**. Interestingly, the crystal structure of **19** (*C*2/*m*; α-phase) has no channels but rather empty cages of 9 Å × 4 Å × 3 Å dimensions connected through narrow 1 Å gaps. Gas molecules must diffuse into the crystal through the narrow gaps. On cooling a crystal of **19** in a CO_2 atmosphere, the crystal underwent a phase transition to a $P\bar{1}$ structure (β-phase) via a slippage manner, generating 1D channels which adsorb CO_2 molecules (Fig. 27b). On cooling to 90 K in the absence of CO_2, the space-group symmetry changes from *C*2/*m* to *C*2/*c* (γ-phase), and the crystal exhibits a similar channel structure with a narrow neck of ca. 2 Å diameter, which is too narrow for atmospheric gas to be adsorbed. However, the *C*2/*c* crystal can smoothly adsorb N_2 gas in the microporous region at 77 K. Likewise, they determined a crystal structure of an O_2-inclusion

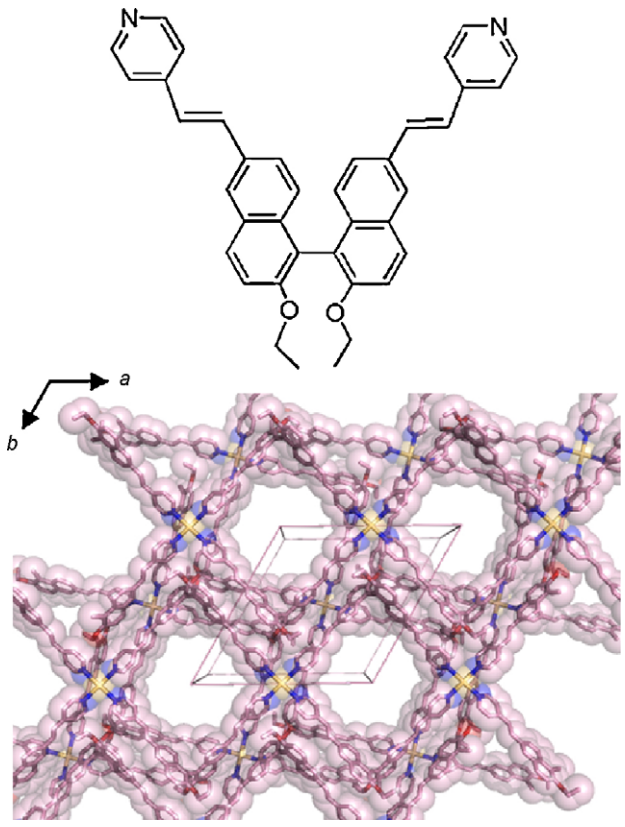

Fig. 26. Crystal structure of the framework of **18** viewed down the *c*-axis. Color code: Cd, yellow; O, red; N, blue; C, pink.

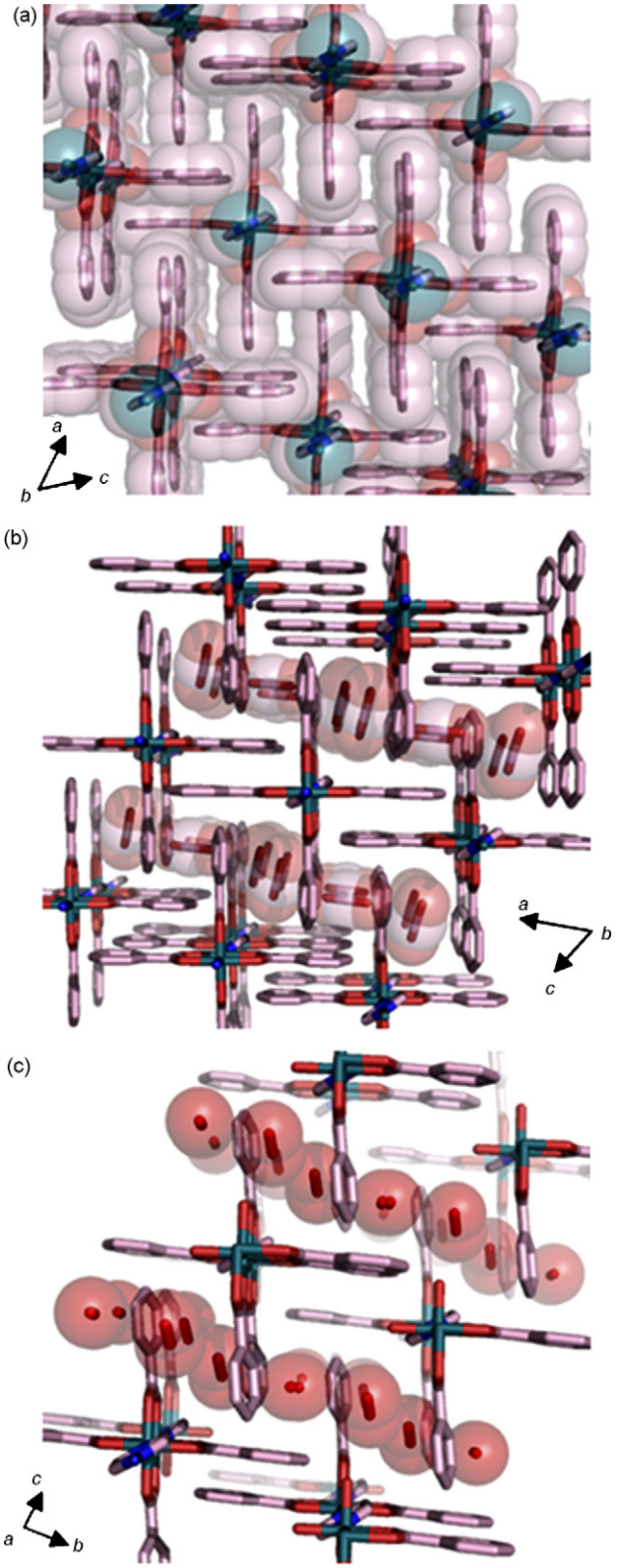

Fig. 27. Crystal structures of (a) **19** under CO_2 atmosphere at 293 K (α-phase), (b) CO_2@**19** at 90 K (β-phase), and (c) O_2@**19** at 10 K.

crystal in which the O–O bond lengths at 10 K were 1.147(17) Å or 1.143(16) Å (Fig. 27c) [32]. Above 90 K O_2 molecules could be modeled, although considerable thermal motion of O_2 was observed. The confined space effectively suppresses the thermal motion of O_2, compared with bulk oxygen in the γ-phase.

Yaghi and co-workers have prepared many fantastic large-pore metal–organic frameworks [33]. In 2005 Yaghi and Howard's group crystallographically determined the primary adsorption sites for Ar and N_2 in network **3** composed of $Zn_4O(CO_2)_6$ connectors and phenylene links. The network has the pores of 12 Å and 15 Å in diameter [34]. Structural refinement at 293 K and 30 K revealed eight symmetry-independent adsorption sites (Fig. 28a). Five of these are sites on the zinc oxide unit and the phenylene link which are the primary adsorption sites $\alpha(CO_2)_3$ for both Ar and N_2 molecules. At temperatures as high as 120 K, significant electron density corresponding to N_2 was observed at these sites. The precise structural information led to atomic level insight into gas-adsorption capability of those sites in the coordination framework.

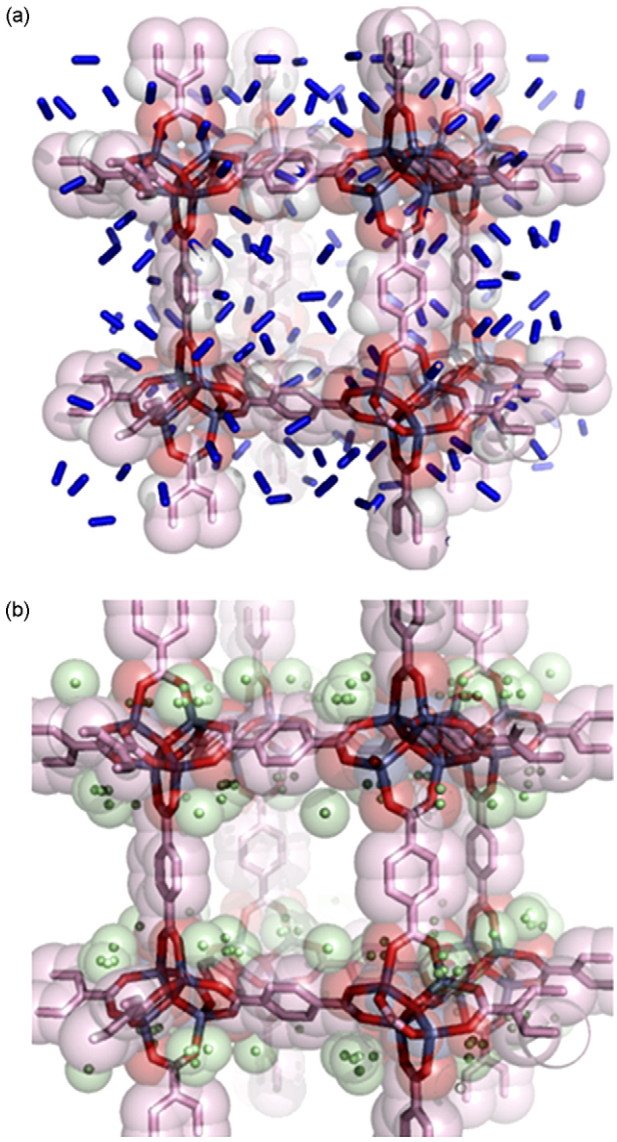

Fig. 28. Gas-inclusion crystal structures: (a) N_2@**3** at 30 K (X-ray diffraction) and (b) H_2@**3** at 5 K (neutron diffraction). Color code: Zn, brown; O, red; N, blue; C, pink; H, green.

Likewise Howard and co-workers succeeded in determining of the hydrogen absorption sites in Zn_4O(1,4-benzenedicarboxylate) by variable temperature (5–300 K) single-crystal Laue neutron diffraction [35]. They carefully determined the gas-inclusion structures and discussed the structural implications cautiously.

The structural analysis revealed that two hydrogen absorption α- and β-sites were found at 5 K, although no hydrogen nuclear density was observed at the β-site at 50 K (Fig. 28b). The α-site is the primary absorption site for Ar and N_2 gas molecules. The shortest framework-gas distances are over 3.1 Å, which is larger than the sum of the van der Waals radii. The structural parameters clearly indicate that the interaction of the hydrogen gas with the electronic potential of the framework is very weak. This study gives a clear picture for hydrogen gas absorption and plenty of implication to other spectroscopic studies as well. This paper also gives general cautions for structural determination analysis using in situ techniques.

5. Concluding remarks

One of the important challenges is to understand the origin of the unique properties of porous coordination networks at atomic level. Tailor-made porous material design requires a structural knowledge of the host–guest interactions. It is essential to have thorough understanding of weak intermolecular interactions for designing/incorporation. In the future, diffraction analysis combined with use of synchrotron radiation will be a powerful tool to better understand guest-inclusion and -exclusion mechanisms due to significantly low noise levels.

Although powder X-ray diffraction (PXRD) studies of coordination networks are beyond the scope, the recent progress of in situ studies should be paid great attention. For example, Kitagawa and co-workers reported fantastic powder work on an acetylene-inclusion structure using a MEM analysis [36]. The huge surface area and the confined channels of the pores within the coordination network can safely adsorb a considerably larger amount of acetylene than the storage limit for an acetylene tank in the absence of an absorber. They determined the array of acetylene molecules in the channels of the framework by PXRD. One can then exhibit the inclusion effects for acetylene in the crystal structure.

As surveyed in this review, the single-crystal-to-single-crystal investigations of coordination networks have emerged in the past decade. There are still not so many in situ crystallographic studies. If the unique features of flexible and robust coordination networks could be fully understood, more object-oriented functional materials could be designed. It is obvious that in situ crystallographic approach can be applicable to analyze dynamic aspects of networks by combination with time-resolved methods capable of providing kinetic information in addition to space. Control of time and space for porous materials will lead to a key technology to realize specific molecular separa-

tions, molecular reactors, catalysis, switchable dynamic solid state systems using porous materials.

References

[1] (a) E.C. Constable, Prog. Inorg. Chem. 42 (1994) 67;
(b) K.R. Dunbar, K.R. Heintz, Prog. Inorg. Chem. (1996) 283;
(c) J.A. Whiteford, E.M. Rachlin, P.J. Stang, Angew. Chem. Int. Ed. 35 (1996) 2524;
(d) S. Batten, R. Robson, Angew. Chem. Int. Ed. 37 (1998) 1460;
(e) P.J. Hagrman, D. Hagrman, J. Zubieta, Angew. Chem. Int. Ed. 38 (1999) 2639;
(f) B. Moulton, M.J. Zaworotko, Chem. Rev. 101 (2001) 1629;
(g) M. Eddaoudi, D.B. Moler, H. Li, B. Chen, T.M. Reineke, M.O. Keeffe, O.M. Yaghi, Acc. Chem. Res. 34 (2001) 319;
(h) S. Kitagawa, R. Kitaura, S.-I. Noro, Angew. Chem. Int. Ed. 43 (2004) 2334;
(i) K. Uermura, S. Kitagawa, Chem. Soc. Rev. 34 (2005) 109.

[2] (a) B.F. Hoskins, R. Robson, J. Am. Chem. Soc. 112 (1990) 1546;
(b) M. Fujita, J. Yazaki, K. Ogura, J. Am. Chem. Soc. 112 (1990) 5645;
(c) M. Fujita, Y.J. Kwon, S. Washizu, K. Ogura, J. Am. Chem. Soc. 116 (1994) 1151.

[3] (a) H. Nakanishi, W. Jones, J.M. Thomas, M.B. Hursthouse, J.M. Motevalli, J. Chem. Soc. Chem. Commun. (1980) 611;
(b) Y. Ohashi, Acta Cryst. A54 (1998) 842;
(c) M. Marchivie, P. Guionneau, J.A.K. Howard, G. Chastanet, J.-F. Letard, A.E. Goeta, D. Chasseau, J. Am. Chem. Soc. 124 (2002) 194;
(d) S. Ohba, H. Hosomi, Y. Ito, J. Am. Chem. Soc. 123 (2001) 6349;
(e) J.R. Scheffer, W. Xia, Top. Curr. Chem. 254 (2005) 233;
(f) J. Harada, H. Uekusa, Y. Ohashi, J. Am. Chem. Soc. 121 (1999) 5809;
(g) P. Coppens, I. Novozhilova, A. Kovalevsky, Chem. Rev. 102 (2002) 861;
(h) M. Irie, S. Kobatake, M. Horichi, Science 291 (2001) 1769;
(i) M. Kawano, K. Hirai, H. Tomioka, Y. Ohashi, J. Am. Chem. Soc. 123 (2001) 6904;
(j) M. Kawano, Y. Kobayashi, T. Ozeki, M. Fujita, J. Am. Chem. Soc. 128 (2006) 6558.

[4] Y. Kobayashi, M. Kawano, M. Fujita, Chem. Commun. (2006) 4377.

[5] C.J. Kepert, M.J. Rossensinsky, Chem. Commun. (1999) 375.

[6] S.S.-Y. Chui, S.M.-F. Lo, J.P.H. Charmant, A.G. Orpen, I.D. Williams, Science 283 (1999) 1148.

[7] H. Li, M. Eddaoudi, M. O'Keeffe, O.M. Yaghi, Nature 402 (1999) 276.

[8] K. Biradha, Y. Hongo, M. Fujita, Angew. Chem. Int. Ed. 39 (2000) 3843.

[9] E. Deiters, V. Bulach, M.W. Hosseini, Chem. Commun. (2005) 3906.

[10] M.P. Suh, J.W. Ko, H.J. Chi, J. Am. Chem. Soc. 124 (2002) 10976.

[11] M.P. Suh, H.R. Moon, E.Y. Lee, S.Y. Jang, J. Am. Chem. Soc. 128 (2006) 4710.

[12] K. Biradha, M. Fujita, Angew. Chem. Int. Ed. 41 (2002) 3392.

[13] Robson, et al., disclosed that **1** with $ZnCl_2$ forms a similar network: S.R. Batten, R. Robson, Angew. Chem. Int. Ed. 37 (1998) 1460.

[14] Note that the space group of **5** changed from $C2/c$ at 193 K to $P2_1/c$ at 80 K, because thermal motions of nitrobenzene were frozen at 80 K.

[15] Later on we reported a 24 Å × 24 Å square ladder complex: O. Ohmori, M. Kawano, M. Fujita, CrystEngComm 6 (2004) 51.

[16] K. Biradha, Y. Hongo, M. Fujita, Angew. Chem. Int. Ed. 41 (2002) 3395.

[17] T.K. Maji, K. Uemura, H.-C. Chang, R. Matsuda, S. Kitagawa, Angw. Chem. Int. Ed. 43 (2004) 3269.

[18] G.J. Halder, C.J. Kepert, J. Am. Chem. Soc. 127 (2005) 7891.

[19] E.Y. Lee, S.Y. Jang, M.P. Suh, J. Am. Chem. Soc. 127 (2005) 6374.

[20] (a) K. Takaoka, M. Kawano, M. Tominaga, M. Fujita, Angew. Chem. Int. Ed. 44 (2005) 2151;
(b) K. Takaoka, M. Kawano, T. Hozumi, S. Ohkoshi, M. Fujita, Inorg. Chem. 45 (2006) 3976.

[21] K. Hanson, N. Calin, D. Bugaris, M. Scancella, S.C. Sevov, J. Am. Chem. Soc. 126 (2004) 10502.

[22] See the crystal structures of these compounds in Ref. [21].

[23] C.-L. Chen, A.M. Goforth, M.D. Smith, C.-Y. Su, H.-C. zur Loye, Angew. Chem. Int. Ed. 44 (2005) 6673.

[24] O. Ohmori, M. Kawano, M. Fujita, J. Am. Chem. Soc. 126 (2005) 16292.

[25] (a) O. Ohmori, M. Kawano, M. Fujita, Angew. Chem. Int. Ed. 44 (2005) 1962;
(b) O. Ohmori, M. Kawano, M. Fujita, CrystEngComm 7 (2005) 255.

[26] G.J. Halder, C.J. Kepert, B. Moubaraki, K. Murray, J.D. Cashion, Science 298 (2002) 1762.

[27] J.-P. Zhang, Y.-Y. Lin, W.-X. Zhang, X.-M. Chen, J. Am. Chem. Soc. 127 (2005) 14162.

[28] C.-D. Wu, W. Lin, Angew. Chem. Int. Ed. 44 (2005) 1958.

[29] (a) M. Kondo, T. Yoshitomi, K. Seki, H. Matsuzaka, S. Kitagawa, Angew. Chem. Int. Ed. Engl. 36 (1997) 1725;
(b) W. Mori, H. Hoshino, Y. Nishimoto, S. Takamizawa, Chem. Lett. (1999) 217;
(c) D. Li, K. Kaneko, Chem. Phys. Lett. 335 (2001) 50.

[30] S. Takamizawa, T. Hiroki, E. Nakata, K. Mochizuki, W. Mori, Chem. Lett. (2002) 1208.

[31] S. Takamizawa, E. Nakata, H. Yokoyama, K. Mochizuki, W. Mori, Angew. Chem. Int. Ed. 42 (2003) 4331.

[32] S. Takamizawa, E. Nakata, T. Saito, Angew. Chem. Int. Ed. 43 (2004) 1368.

[33] K.S. Park, Z. Ni, A.P. Côté, J.Y. Choi, R. Huan, F.J. Uribe-Romo, H.K. Chae, M. O'Keeffe, O.M. Yaghi, PNAS 103 (2006) 10186.

[34] J.L.C. Rowsell, E.C. Spencer, J. Eckert, J.A.K. Howard, O.M. Yaghi, Science 309 (2005) 1350.

[35] E.C. Spencer, J.A.K. Howard, G.J. McIntyre, J.L.C. Rowsell, O.M. Yaghi, Chem. Commun. (2006) 278.

[36] R. Matsuda, R. Kitaura, S. Kitagawa, Y. Kubota, R.V. Belosludov, T.C. Kobayashi, H. Sakamoto, T. Chiba, M. Takata, Y. Kawazoe, Y. Mita, Nature 436 (2005) 238.